Supplemental Data for:

Enzyme Inhibition by Allosteric Capture of an Inactive Conformation

Gregory M. Lee[1], Tina Shahian[2], Aida Baharuddin[1],
Jonathan E. Gable[3], and Charles S. Craik[1]*

[1] Department of Pharmaceutical Chemistry
University of California
San Francisco, CA 94158-2280
USA

[2] Graduate Group in Biochemistry and Molecular Biology
University of California
San Francisco, CA, 94158-2280
USA

[3] Graduate Group in Biophysics
University of California
San Francisco, CA, 94158-2280
USA

*Correspondence should be addressed to C.S.C. (craik@cgl.ucsf.edu)

SUPPLEMENTAL DATA TABLE OF CONTENTS

Movie S1-S3 Captions: Morph animations ……... 3

Fig. S1: ^{15}N-^{1}H HSQC spectra of KSHV Pr truncations ……..……..... 4

Fig. S2: ^{13}C-^{1}H HSQC spectra of KSHV Pr truncations ……... 5

Fig. S3: ^{13}C-^{1}H HSQC spectra of the Ile-to-Val mutants …….. 6

Fig. S4: DD2 titration of KSHV Pr M197D-I201V …….. 8

Fig. S5: The alternative conformation of the KSHV Pr Δ196-DD2 complex ……. 9

Fig. S6: *In situ* DD2 F_o-F_c omit maps …….. 11

Fig. S7: The conformations of KSHV Pr-bound DD2 …… 12

Table S1: Overall average B-values: KSHV Pr Δ196-DD2 ……. 13

Table S2: Structural comparison of KSHV Pr constructs ……..... 13

Table S3: Average sidechain B-values of residues ≤ 5 Å to DD2 ……... 14

Table S4: Structural comparison of KSHV Pr-bound DD2 conformations …… 15

Table S5: Selected KSHV Pr Δ196 residue-DD2 sidechain interatomic distances….. 16

Table S6: Average sidechain B-values of the active-site residues …… 17

Table S7: DD2 solubility and cell permeability ……. 18

Table S8: Structural comparison of HHV Pr monomers vs. KSHV Pr…… 18

References ……..... 19

Movie S1. KSHV Pr dimer with the dimer interface and C-terminal truncations. A rotation of the KSHV Pr dimer (2PBK) focusing on the dimer interface, including the C-terminal α-helices 5 and 6. The animation also displays the positions of the C-terminal truncations.

Movie S2. DD2 pocket morph of the KSHV Pr monomeric units from apo to DD2-bound states. A morph modeling the structural transition of a monomeric unit of the KSHV Pr dimer (2PBK) to the KSHV Pr Δ196-DD2 complex (3NJQ), focusing on the allosteric DD2 binding pocket. Residues 197-230 of 2PBK are omitted for clarity.

Movie S3. Active site morph of the KSHV Pr monomeric units from apo to DD2-bound states. A morph modeling the structural transition of a monomeric unit of the KSHV Pr dimer (2PBK) to the KSHV Pr Δ196-DD2 complex (3NJQ), focusing on the active site. Residues 197-230 of 2PBK are omitted for clarity.

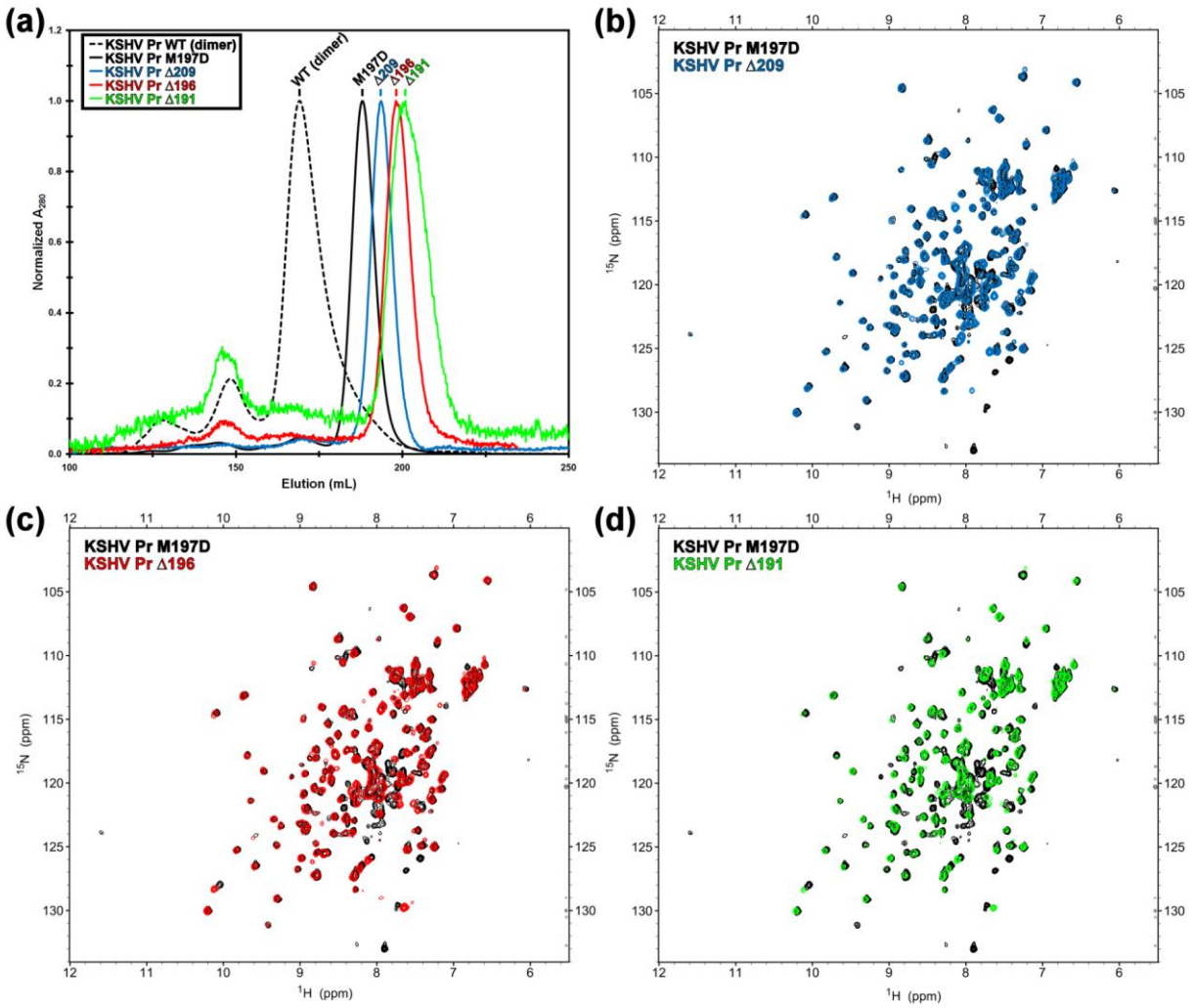

Figure S1. The ^{15}N-^{1}H HSQC spectra of KSHV Pr truncations. (**a**) Size exclusion chromatograms of the KSHV Pr truncations (Δ209, blue; Δ196, red; Δ191 green) indicate that each elute as monomers. Wild-type KSHV Pr dimer (dashed black) and the obligate M197D monomer (solid black) are presented as references. The peaks eluting less than 150 mL indicate unidentified oligomeric species. Overlays of the ^{15}N-^{1}H HSQC spectra of uniformly ^{15}N-labeled KSHV Pr M197D and Δ209 (**b**), Δ196 (**c**), and Δ191 (**d**) indicate no significant structural perturbations of the core protein backbone upon truncation of the conformationally dynamic C-terminal residues.

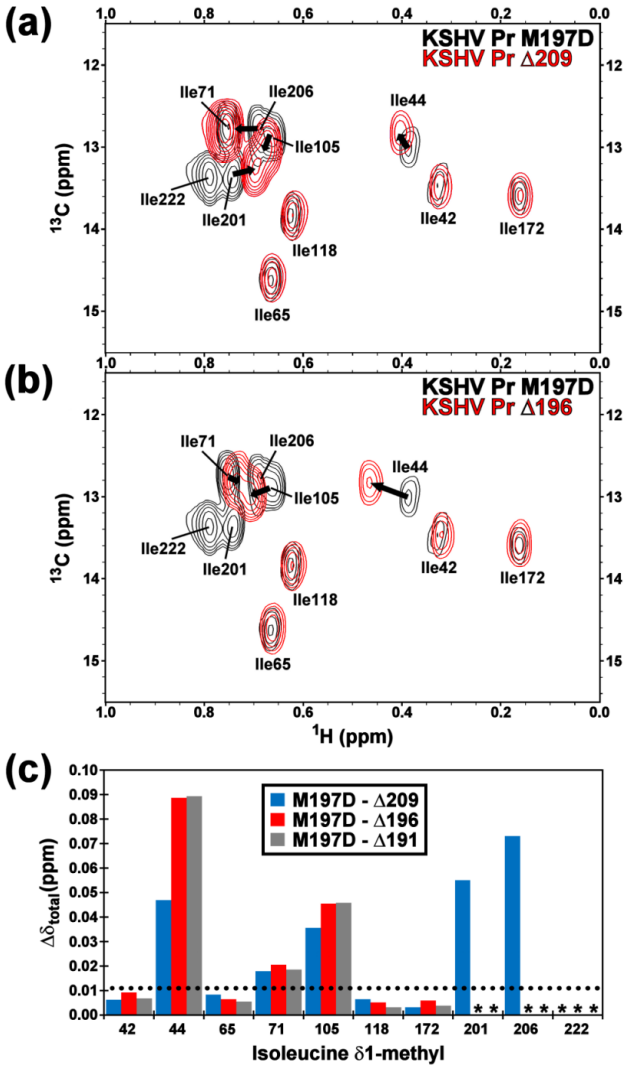

Figure S2. ^{13}C-^{1}H HSQC spectra of KSHV Pr truncations. The ^{13}C-^{1}H HSQC spectra focusing on the isoleucine δ1-methyl resonances of selective [^{13}C-^{1}H methyl] ILV labeled KSHV Pr M197D (black) superimposed with those of Δ209 (**a**, red) and Δ196 (**b**, red). No significant spectral differences are observed between the Δ196 and Δ191 constructs (not shown). (**c**) Combined chemical shift perturbations between the full-length monomer and truncated KSHV Pr constructs > 0.01 ppm (dotted line) clearly identify the interfacial (Ile44 and Ile105) and C-terminal (Ile201, Ile206, and Ile222) residues. Asterisks indicate no isoleucine residue present in the selected truncation.

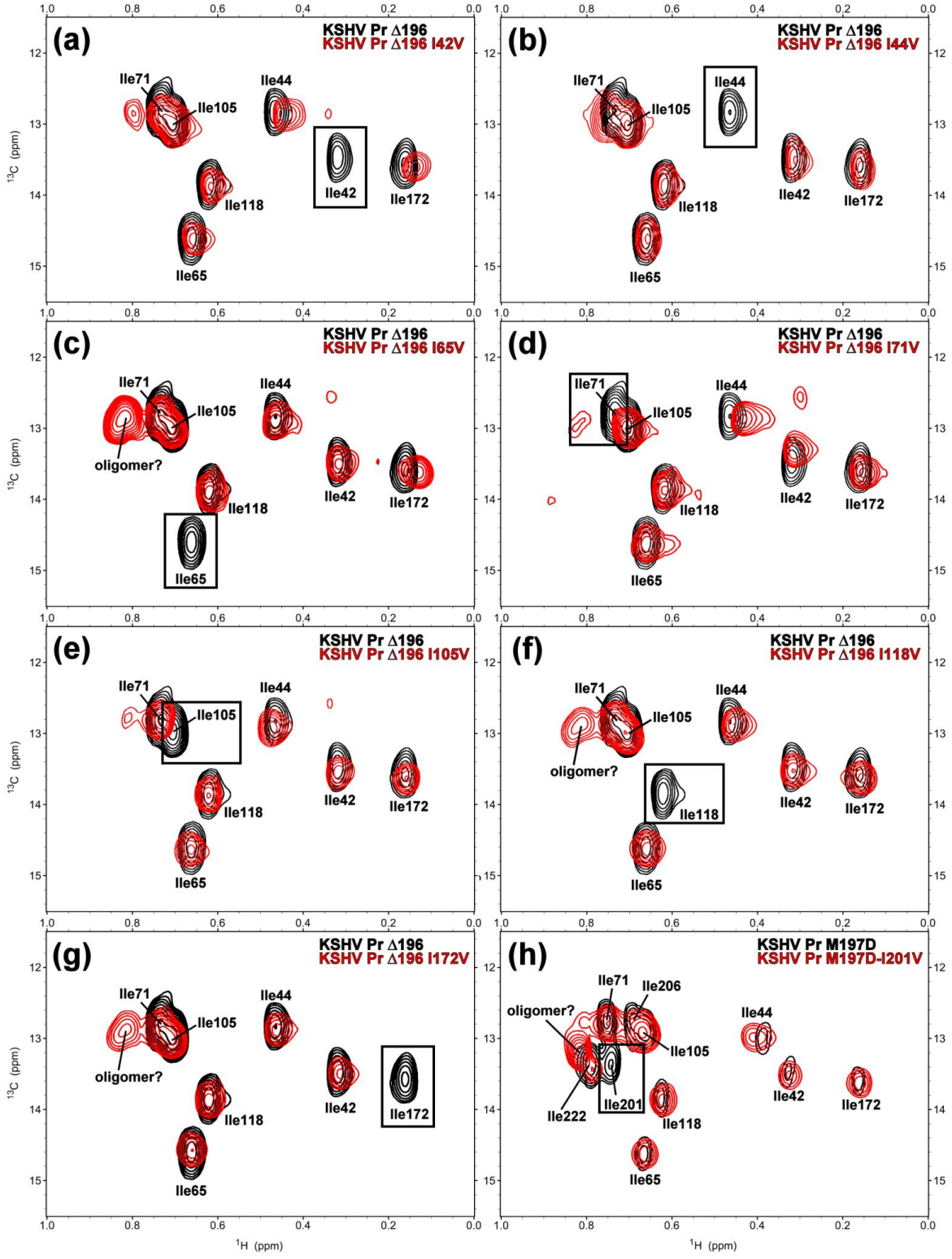
(a)
KSHV Pr Δ196
KSHV Pr Δ196 I42V
(b)
KSHV Pr Δ196
KSHV Pr Δ196 I44V
(c)
KSHV Pr Δ196
KSHV Pr Δ196 I65V
(d)
KSHV Pr Δ196
KSHV Pr Δ196 I71V
(e)
KSHV Pr Δ196
KSHV Pr Δ196 I105V
(f)
KSHV Pr Δ196
KSHV Pr Δ196 I118V
(g)
KSHV Pr Δ196
KSHV Pr Δ196 I172V
(h)
KSHV Pr M197D
KSHV Pr M197D-I201V
Ile71
Ile105
Ile44
Ile42
Ile172
Ile118
Ile65
oligomer?
Ile206
Ile222
Ile201
^{13}C (ppm)
^{1}H (ppm)

Figure S3. The ^{13}C-^{1}H HSQC spectra of the Ile-to-Val mutants. Significant aggregation of the KSHV Pr obligate monomer at high protein concentrations precluded the acquisition of triple-resonance experiments typically used to assign resonances. Therefore, Ile-to-Val mutations were performed to assign the Ile δ1-methyl groups. Overlays of the ^{13}C-^{1}H HSQC spectra of these mutants (**a-h**, as indicated) suggest no significant structural perturbations relative to the "wild-type" constructs. Missing resonances (boxed) indicate the identity of the Ile-to-Val mutation. The Ile222 peak was identified by comparing the spectra of full-length KSHV Pr M197D and the Δ209 construct (**Fig. S2**). The Ile206 peak was identified through a process of elimination. The respective ^{15}N-^{1}H HSQC spectra (not shown) display no significant resonance perturbations relative to the full-length KSHV Pr M197D construct.

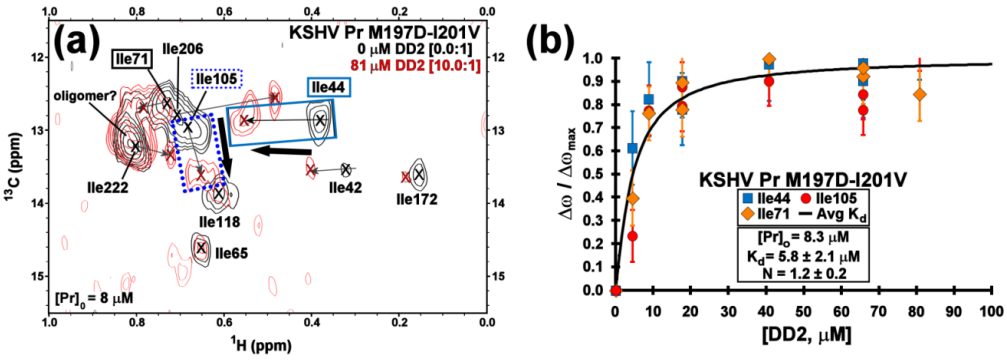

Figure S4. DD2 titration of KSHV Pr M197D-I201V. (**a**) The ^{13}C-^{1}H HSQC titration spectra of the KSHV Pr M197D-I201V construct with DD2. The spectral overlays display apo (black) and > 5 molar equivalents DD2 (red), and are focused on the isoleucine δ1-methyl region. Ile44 (solid blue box), Ile105 (dotted blue box), and Ile71 (solid black box) are used as the binding probes. (**b**) The binding curve represents the average of the Hill equation-derived apparent K_d values calculated for the three probes (symbols as indicated). Comparisons with the M197D and Δ196 constructs are illustrated in **Figure 2**.

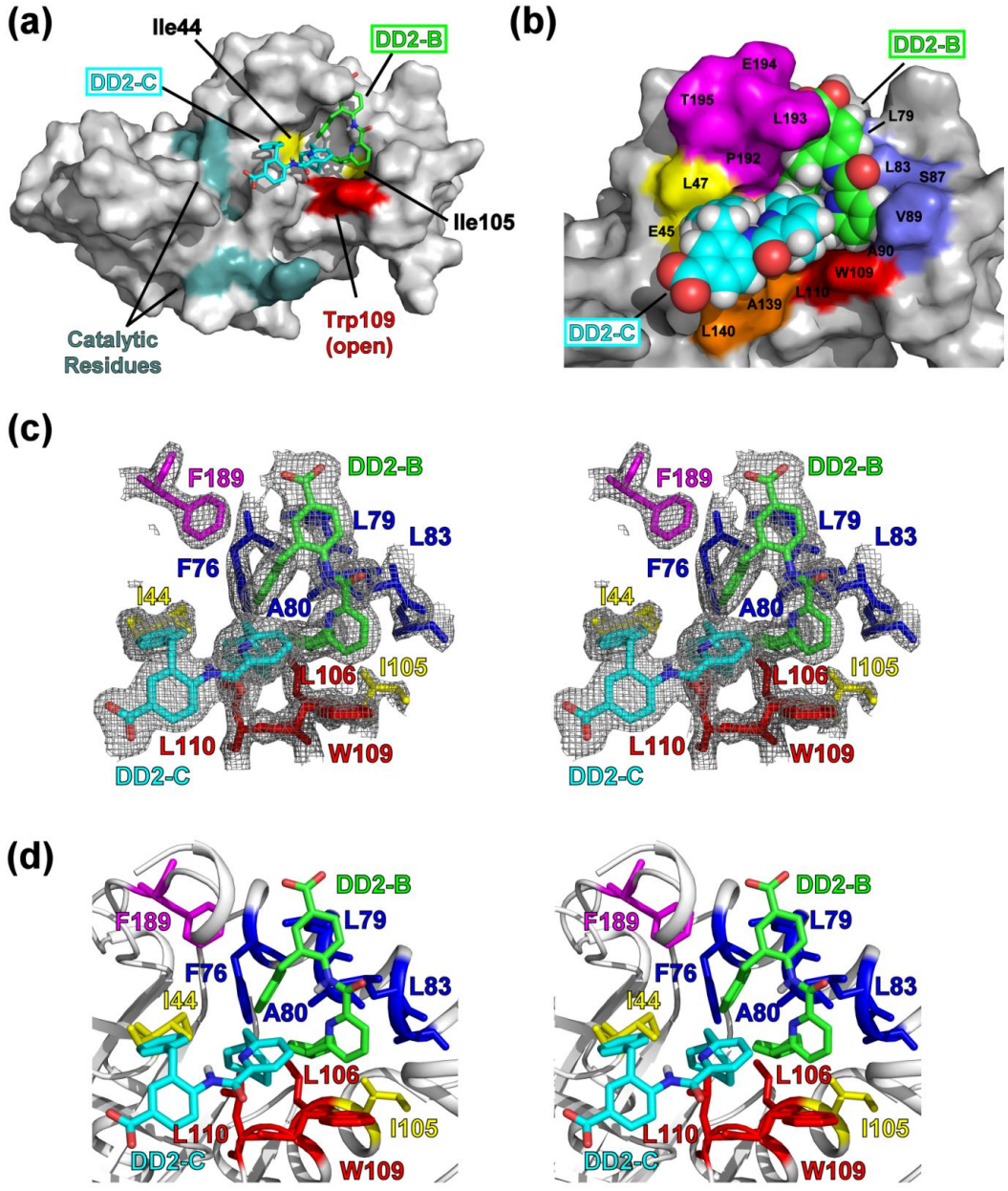
(a)
Ile44
DD2-B
DD2-C
Ile105
Catalytic Residues
Trp109 (open)
(b)
DD2-B
E194
T195
L193
L79
P192
L83
S87
L47
V89
E45
A90
W109
L110
A139
DD2-C
L140
(c)
F189
DD2-B
L79
L83
F76
I44
A80
L106
I105
L110
W109
DD2-C
(d)

Figure S5. The alternate conformation of the KSHV Pr Δ196-DD2 complex. (**a**) Monomer B of the KSHV Pr Δ196-DD2 complex contains two DD2 molecules (DD2-B, green carbons; DD2-C, cyan carbons). DD2-C is located outside the binding pocket and may act as a "bridging" molecule between crystallographic unit cells. (**b**) The hydrophobic DD2 binding pocket is composed of aliphatic residues from the β2-β3 loop (yellow), helix 1 and the α1-α2 loop (blue), helix 2 (red), the β6-β7 loop (orange), and the C-terminus (magenta). DD2-B (green carbons) and DD2-C (cyan carbons) of DD2 are shown as space filling models. (**c**) Stereoview of DD2-B (green) and DD2-C (cyan) within the Δ196 binding pocket of monomer B, in relation to the "hot spot" Trp109 (red) and the Ile44 and Ile105 reporter groups (yellow). Also displayed are the buried aliphatic residues of helix 1 (blue), helix 2 (red), and the C-terminus (magenta) that compose the binding pocket. The mesh represents the $2F_o$-F_c 1σ electron density map. (**d**) **Figure S5c** with the protein backbone ribbons displayed. These figures are comparable to **Figures 4** and **5**.

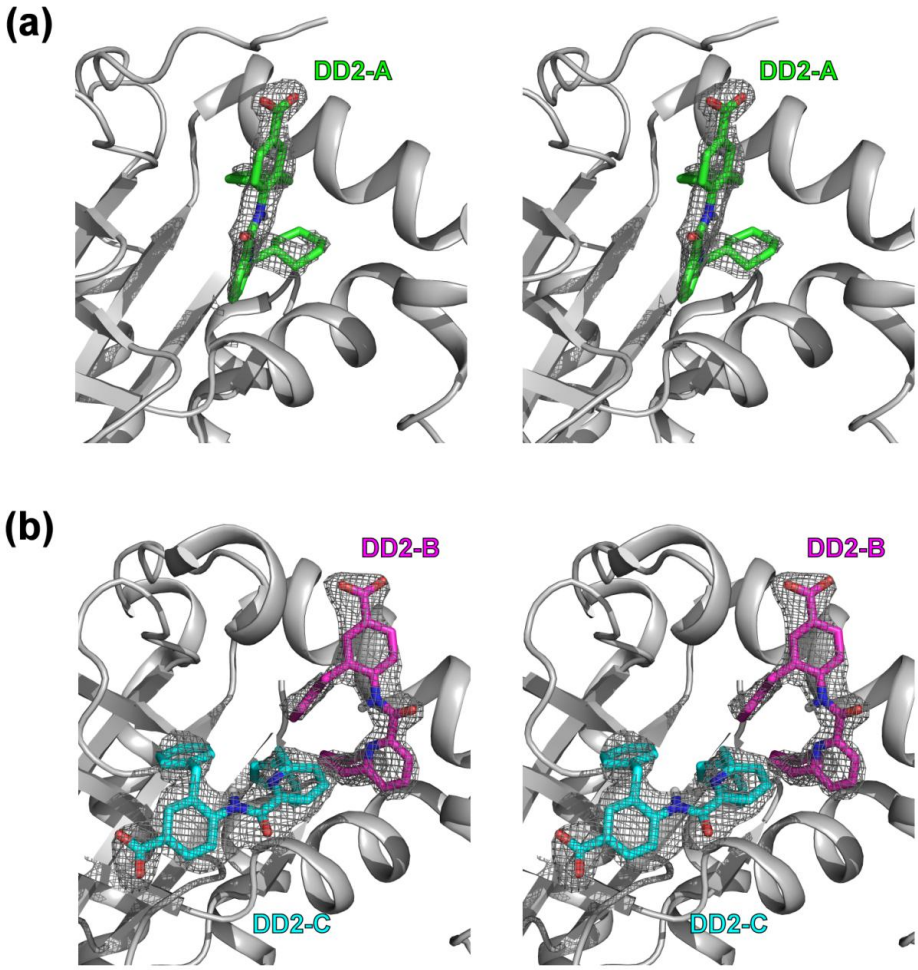

Figure S6. *In situ* DD2 F_o-F_c omit maps. (**a**) A stereoview of the KSHV Pr Δ196-DD2 monomer A. The mesh surrounding DD2-A (green carbons) represents the F_o-F_c omit map contoured at 3.0σ. (**b**) A stereoview of the KSHV Pr Δ196-DD2 monomer B. The mesh surrounding DD2-B (magenta carbons) and DD2-C (cyan carbons) represents the F_o-F_c omit map contoured at 3.0σ.

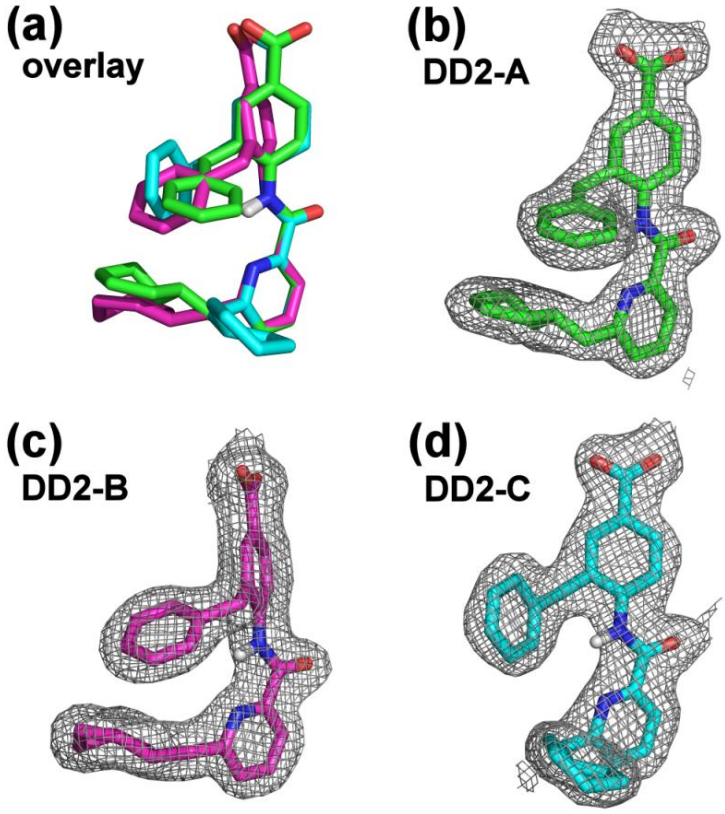

Figure S7. The poses of KSHV Pr-bound DD2. (**a**) The superimposed DD2 crystal structures (DD2-A, green carbons; DD2-B, magenta carbons; DD2-C, cyan carbons) exhibit distinct conformers. Shown are the $2F_o$-F_c 1σ electron density images of the three poses of the DD2 bound to the KSHV Pr Δ196 construct: DD2-A (**b**, green) in monomer A; DD2-B (**c**, magenta) and DD2-C (**d**, cyan) in monomer B. The structures of the KSHV Pr Δ196 construct are omitted for clarity.

TABLE S1.
AVERAGE B-VALUES: KSHV PR Δ196-DD2

KSHV Pr Δ196-DD2 complex	Monomer A (Å^2)	Monomer B (Å^2)
Backbone heavy atoms	49.1	40.2
Sidechain heavy atoms	52.8	43.7
All heavy atoms	50.9	41.9

TABLE S2.
STRUCTURAL COMPARISON OF KSHV PR CONSTRUCTS

Overlay (residues 1-196)	[a]RMSD Backbone Atoms (Å)	[a]RMSD Heavy Atoms(Å)
2PBK (A) vs. Δ196-DD2 (A)	0.77	0.89
2PBK (A) vs. Δ196-DD2 (B)	0.77	0.95
1FL1 (B) vs. Δ196-DD2 (A)	0.60	0.74
1FL1 (B) vs. Δ196-DD2 (B)	0.60	0.77
Δ196-DD2 monomer A vs B	0.52	0.61

[a]RMSD calculations performed using Pymol 1.2 (Schrödinger, LLC).
2PBK = peptide-phosphonate inhibited KSHV Pr dimer[1]
1FL1 = apo KSHV Pr dimer[2]
3NJQ = KSHV Pr Δ196-DD2 complex, **this study.**

TABLE S3.
AVERAGE [a] SIDECHAIN B-VALUES OF RESIDUES ≤ 5 Å TO DD2

[b] DD2-A & DD2-B (inhibitors)				[b] DD2-C (bridging molecule)		
Residue	Monomer A ($Å^2$)	Monomer B ($Å^2$)		Residue	Monomer A ($Å^2$)	Monomer B ($Å^2$)
Phe 76	26.3	28.4		Glu 45	n/a	31.4
Leu 79	30.0	36.2		Leu 47	n/a	34.4
Ala 80	26.7	28.8		Trp 109	n/a	24.7
Leu 83	29.2	29.8		Leu 110	n/a	23.4
Val 89	28.5	34.4		Ala 139	n/a	30.4
Ala 90	26.3	27.3		Leu 140	n/a	30.9
Trp 109	**28.6**	**24.7**		Arg 144	n/a	47.3
Leu 110	25.0	23.4				
Ala 139	36.5	30.4				
Leu140	48.7	30.9				
Phe 189	32.6	33.7				
Pro 192	44.9	37.2				
Leu 193	50.7	39.3				
Glu 194	[c]	53.1				
[d] Average	34.2	32.6		[d] Average	n/a	32.0
Stdev.	9.5	8.1		Stdev.	n/a	9.5
[e] Overall Average	33.4			Overall Average [d]	47.3	
Stdev.	8.8			Stdev.	18.0	

[a] Includes Cα atom.
[b] DD2-A = 3NJQ A 197; DD2-B = 3NJQ B 198; DD2-C = 3NJQ B 199
[c] Electron density maps of Glu194 – Leu 196 not observed for 3NJQ monomer A.
[d] Average and standard deviation of the individual monomers.
[e] Overall average and standard deviation of the dimer.

TABLE S4.
STRUCTURAL COMPARISON OF KSHV PR-BOUND DD2 CONFORMATIONS

DD2 Overlay	[a]RMSD (Å) all atoms	[a]RMSD (Å) all hv atoms	[a]RMSD (Å) [b]backbone	[a]RMSD (Å) [b]backbone+ [c]sidechain 1	[a]RMSD (Å) [b]backbone+ [d]sidechain 2
[e] A vs. B	1.91	1.12	0.51	0.86	1.03
[e] A vs. C	1.99	0.53	0.34	0.85	0.36
[e] B vs. C	3.12	2.43	0.67	1.74	0.98

[a] RMSD calculations performed using Pymol 1.2 (Schrödinger, LLC).
[b] DD2 backbone = 4-(pyridine-2-amido) benzoic acid.
[c] Sidechain 1 = cyclohexyl methylenyl group
[d] Sidechain 2 = benzyl group
[e] DD2-A = 3NJQ A 197; DD2-B = 3NJQ B 198; DD2-C = 3NJQ B 199

DD2 pose # (Monomer ID)	[f]Amide H-pyridine N distance (Å)	[f]Amide N-pyridine N dihedral angle (^{o})
DD2-A (A 197)	2.1 Å	-7.0^o
DD2-B (B 198)	2.2 Å	-4.9^o
DD2-C (B 199)	2.2 Å	-9.7^o

[f] Measurements performed using Pymol 1.2 (Schrödinger, LLC).

TABLE S5.
SELECTED KSHV PR Δ196- DD2 SIDECHAIN INTERATOMIC DISTANCES (Å)

[a]DD2 atom #	Δ196 residue	Atom	[b]Monomer A (Å)	[c]Monomer B (Å)
#27 (benzyl ring)	Ile 44	Cδ1	3.8	5.8
	Phe 76	Cδ / Cε / Cζ	3.7 / 3.6 / 4.9	4.7 / 4.1 / 5.1
	Leu 79	Cδ1 / Cδ2	4.4 / 5.1	5.0 / 6.1
	Leu 83	Cδ1 / Cδ2	6.3 / 8.5	4.9 / 7.2
	Phe 189	Cδ / Cε / Cζ	4.9 / 3.8 / 3.7	7.3 / 6.0 / 5.5
	Pro 192	Cβ / Cγ / Cδ	7.4 / 6.0 / 5.9	5.6 / 4.4 / 4.5

[a]DD2 atom #	Δ196 residue	Atom	[b]Monomer A (Å)	[c]Monomer B (Å)
#11 (cyclohexyl)	Ile 44	Cδ1	8.5	7.8
	Phe 76	Cδ / Cε / Cζ	7.1 / 6.1/ 6.1	6.3 / 5.2 / 5.0
	Ala 80	Cβ	4.5	4.0
	Leu 83	Cδ1 / Cδ2	4.3 / 6.4	5.2 / 7.0
	Ala 90	Cβ	4.9	6.3
	Ile 105	Cγ2 / Cδ1	3.7 / 7.0	3.8 / 6.9
	Leu 106	Cδ1 / Cδ2	5.0 / 7.2	3.7 / 5.9
	Trp 109	Cβ	5.4	5.1
	Leu 110	Cδ1 / Cδ2	6.5 / 7.6	5.0 / 6.5

[a] DD2 numbering performed using ACD ChemSketch 12.0.
[b] DD2-A to monomer A residues;
[c] DD2-B to monomer B residues.

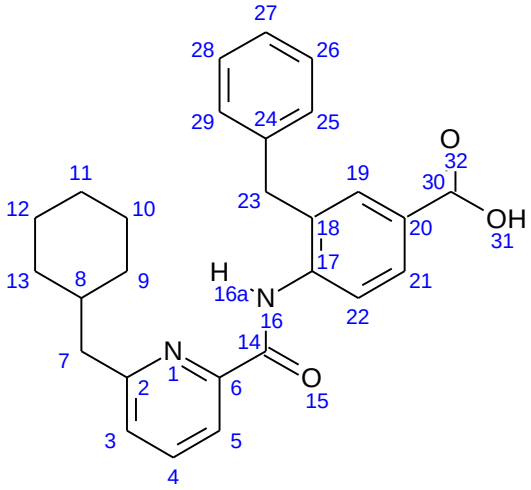

TABLE S6.
AVERAGE [a]SIDECHAIN B-VALUES OF THE ACTIVE-SITE RESIDUES

	Catalytic Triad	
Residue	Monomer A (Å^2)	Monomer B (Å^2)
His 46	32.3	36.1
Ser 114	35.8	31.8
His 134	32.8	32.9
Average	33.3	34.0
Stdev.	2.1	2.8

β1-α0 loop (residues 14-27)				**β6-β7 loop (residues 139-149)**		
Residue	Monomer A (Å^2)	Monomer B (Å^2)		Residue	Monomer A (Å^2)	Monomer B (Å^2)
Val 14	43.8	35.7		Cys 138	34.1	31.6
Ser 15	52.9	48.4		Ala 139	36.5	30.4
Cys 16	52.9	53.2		Leu 140	48.7	30.9
Pro 17	45.9	61.2		Gly 141	54.9	34.6
Lys 18	52.3	77.7		[b]**Arg 142**	**59.4**	**36.0**
Leu 19	61.7	81.0		[b]**Arg 143**	**75.6**	**41.0**
Glu 20	86.6	66.8		Arg 144	84.4	47.3
Gln 21	73.8	54.1		Gly 145	63.3	32.4
Glu 22	58.3	41.9		Thr 146	60.4	26.6
Leu 23	64.4	47.0		Val 147	45.9	27.1
Tyr 24	55.7	33.8		Ala 148	38.0	26.0
Leu 25	54.9	41.7		Val 149	40.5	30.2
Asp 26	75.5	50.2				
Pro 27	64.0	42.7				
[c]Average	61.0	52.3		[c]Average	59.1	35.2
Stdev.	12.1	15.1		Stdev.	17.1	8.3
[d]Overall Average	56.6			[d]Overall Average	47.3	
Stdev.	14.3			Stdev.	18.0	

[a] Includes Cα atom.
[b] Oxyanion hole-stabilizing residues.
[c] Average and standard deviation of the individual monomers.
[d] Overall average and standard deviation of the dimer.

TABLE S7.
DD2 SOLUBILITY AND CELL PERMEABILITY

	[a]Solubility (μM)	[b]Permeability (10^{-6} cm s^{-1})	[c]Retention (%)
DD2	0.49	296	91

[a] Solubility in PBS buffer (pH 7.4) containing 1% DMSO
[b,c] Permeability/retention across an artificial membrane (PAMPA), pH 7.4

TABLE S8.
STRUCTURAL COMPARISON OF [a]HHV PR MONOMERS VS KSHV PR

[b]Overlay, all residues	HHV Pr subfamily	PDB accession code	[b,c]RMSD Backbone Atoms (Å)	[b,c]RMSD Heavy Atoms (Å)
HSV-2 Pr	Alpha	1AT3	1.11	1.38
VZV Pr	Alpha	1VZV	1.09	1.34
HCMV Pr	Beta	1CMV	0.75	0.82
EBV Pr	Gamma	1O6E	0.95	1.17

[a] No PDB files are currently available for HSV-1 Pr, HHV-6 Pr and HHV-7 Pr.
[b] Overlay of monomer A from each PDB file onto KSHV Pr monomer A (2PBK)
[c] RMSD calculations performed using Pymol 1.2 (Schrödinger, LLC).

REFERENCES

1. Lazic, A., Goetz, D. H., Nomura, A. M., Marnett, A. B. & Craik, C. S. (2007). Substrate Modulation of Enzyme Activity in the Herpesvirus Protease Family. *J Mol Biol* **373**, 913-923.
2. Reiling, K. K., Pray, T. R., Craik, C. S. & Stroud, R. M. (2000). Functional consequences of the Kaposi's sarcoma-associated herpesvirus protease structure: regulation of activity and dimerization by conserved structural elements. *Biochemistry* **39**, 12796-803.